

Unique Antiplatelet Effects of a Novel S-Nitrosoderivative of a Recombinant Fragment of von Willebrand Factor, AR545C: In Vitro and Ex Vivo Inhibition of Platelet Function

By Aida Inbal, Osnat Gurevitz, Ilia Tamarin, Regina Eskaraev, Angela Chetrit, Ilia Novicov, Monica Feldman, David Varon, Michael Eldar, and Joseph Loscalzo

The recombinant fragment of von Willebrand factor (vWF) spanning Ala444 to Asp730 and containing an Arg545Cys mutation (denoted AR545C) has antithrombotic properties that are principally a consequence of its ability to inhibit platelet adhesion to subendothelial matrix. Endothelial-derived nitric oxide (NO) can also inhibit platelet function, both as a consequence of inhibiting adhesion as well as activation and aggregation. Nitric oxide can react with thiol functional groups in the presence of oxygen to form S-nitrosothiols, which are naturally occurring NO derivatives that prolong the biological actions of NO. Because AR545C has a single free cysteine (Cys545), we attempted to synthesize the S-nitroso-derivative of AR545C and to characterize its antiplatelet effects. We successfully synthesized S-nitroso-AR545C and found that it contained 0.96 mol S-NO per mole peptide. S-nitroso-AR545C was approximately 5-fold more potent at inhibiting platelet agglutination than was the unmodified peptide ($IC_{50} = 0.02 \pm 0.006 \mu\text{mol/L}$ v $0.1 \pm 0.03 \mu\text{mol/L}$, $P = .001$). In addition and by contrast, S-nitroso-AR545C was a powerful inhibitor of adenosine diphosphate-induced platelet aggregation ($IC_{50} = 0.018 \pm 0.002 \mu\text{mol/L}$), while AR545C had no effect on aggregation. These effects

were confirmed in studies of adhesion to and aggregation on extracellular matrix under conditions of shear stress in a cone-plate viscometer, where $1.5 \mu\text{mol/L}$ S-nitroso-AR545C inhibited platelet adhesion by 83% and essentially completely inhibited aggregate formation, while the same concentration of AR545C inhibited platelet adhesion by 74% and had significantly lesser effect on aggregate formation on matrix ($P \leq .004$ for each parameter by ANOVA). In an ex vivo rabbit model, we also found that S-nitroso-AR545C had a more marked and more durable inhibitory effect on botrocetin-induced platelet aggregation than did AR545C, and these differences were also reflected in the extent and duration of effect on the prolongation of the bleeding time in these animals. These data show that S-nitroso-AR545C has significant and unique antiplatelet effects, inhibiting both adhesion and aggregation, by blocking platelet GPIIb/IIIa receptor through the AR545C moiety and elevating platelet cyclic 3',5'-guanosine monophosphate through the -SNO moiety. These observations suggest that this NO-modified fragment of vWF may have potential therapeutic benefits as a unique antithrombotic agent.

© 1999 by The American Society of Hematology.

VON WILLEBRAND FACTOR (vWF) is a multimeric glycoprotein synthesized by megakaryocytes and endothelial cells, and is released both into the circulation and the subendothelial space.¹ At sites of vascular injury, platelet activation is initiated by interactions of vWF and a specific receptor on platelets, glycoprotein Ib (GPIb). The interaction of vWF with GPIb is critical for the initiation of platelet deposition, both during normal hemostasis² and in the setting of arterial thrombosis.³⁻⁵ This initial hemostatic effect is triggered by vWF associated with subendothelial matrix, and is modulated by shear stress evoked by flowing blood in the vasculature. Platelet aggregation is then further promoted by activation of another platelet receptor complex, glycoprotein IIb/IIIa (GPIIb/IIIa), leading to the binding of fibrinogen or vWF to the platelet surface.⁶

The A1 domain of the vWF molecule is known to contain the GPIIb-binding site, first assigned to a tryptic fragment spanning amino acids 449 to 728 that contains a large intrachain disulfide-linked (Cys509-Cys695) loop.^{7,8} The pharmacological inhibition of the high shear stress-induced platelet adhesion to vWF with monoclonal anti-vWF antibodies,^{5,9} aurin tricarboxylic acid,^{10,11} or the recombinant A1 domain fragment VCL¹² reduces thrombus formation in various animal models, emphasizing the crucial role vWF plays in arterial thrombogenesis.

We recently reported that the recombinant vWF fragment spanning Ala444 to Asp730 and containing an Arg545Cys mutation, denoted AR545C, has antithrombotic properties in vitro and in vivo.¹³ AR545C is a gain of function mutation that results in an increased and also spontaneous binding of the fragment to platelet GPIIb,¹³ thereby blocking the initial interac-

tion between native vWF and platelet GPIIb, preventing any further process of platelet activation. Indeed, the mutated AR545C fragment inhibited ristocetin- and botrocetin-induced platelet agglutination of human and rabbit platelets, respectively, and enhanced the thrombolytic effect of recombinant tissue-type plasminogen activator in a rabbit thrombosis model.¹³

Endothelium-derived nitric oxide (NO) inhibits platelet aggregation^{14,15} and prevents adhesion of platelets to the subendothelium,¹⁶ and does so in association with elevating intracellular cyclic 3',5'-guanosine monophosphate (cGMP). NO is stabilized by reacting with sulfhydryl groups in the presence of oxygen to form S-nitrosothiols, thereby prolonging its half-life and preserving its biological activity.¹⁷ The AR545C molecule

From the Institutes of Thrombosis and Hemostasis, Neufeld Cardiac Research Institute, and Clinical Epidemiology, Sackler School of Medical, Sheba Medical Center, Tel-Hashomer, Israel; and the Whitaker Cardiovascular Institute and Evans Department of Medicine, Boston University School of Medicine, Boston, MA.

Submitted October 26, 1998; accepted May 10, 1999.

Supported in part by National Institutes of Health (NIH) Grants No. HL53919, HL48743, HL53993, and by a Merit Review Award from the US Veterans Administration.

Address reprint requests to Aida Inbal, MD, Institute of Thrombosis & Hemostasis, Sheba Medical Center, Tel-Hashomer 52621, Israel.

The publication costs of this article were defrayed in part by page charge payment. This article must therefore be hereby marked "advertisement" in accordance with 18 U.S.C. section 1734 solely to indicate this fact.

© 1999 by The American Society of Hematology.

0006-4971/99/9405-0035\$3.00/0

contains 3 cysteine residues involved in interchain bonds (residues 459, 461, and 464), 2 pairs of intrachain disulfide bonds (residues 471-474 and 509-695), and 1 apparently free cysteine (residue 545).¹⁸ S-nitrosation of AR545C (S-nitroso-AR545C) at Cys545 should, therefore, endow the molecule with potent and long-lasting NO-like effects. This compound may be of potential clinical interest because 2 independent antiplatelet activities are combined in the same molecule, viz, antiadhesive and antiaggregatory effects. The aim of the present study is to synthesize and characterize the antiplatelet effects of S-nitroso-AR545C in vitro and ex vivo, and to compare these effects to the parent peptide AR545C.

MATERIALS AND METHODS

Construction, synthesis, and purification of the peptide AR545C. The sequence encoding alanine 444-asparagine 730 and containing the arginine-to-cysteine substitution at amino acid residue 545 (AR545C) was derived from a full-length cDNA for human vWF.¹³ The coding sequence was inserted into a pZEM229 expression vector and expressed in a thymidine kinase-deficient BHK cell line, BHK-570, using methotrexate for growth selection as previously described.¹³ The AR545C peptide was purified from the BHK media by heparin-Sepharose CL-6B affinity chromatography (Pharmacia Biotech, Piscataway, NJ), yielding essentially pure material. The purity of the peptide was verified by sodium dodecyl sulfate-polyacrylamide gel electrophoresis (SDS-PAGE) under nonreducing or reducing conditions, as well as by reverse-phase high-performance liquid chromatography with a Vydac C8 column (Vydac, Hesperia, CA).¹³ The amount of the peptide was quantified by a sandwich enzyme-linked immunosorbent assay (ELISA) using 1:100 rabbit anti-human vWF (Dakopatts A082; Dako, Glostrup, Denmark) as the coating antibody and 1:1,000 peroxidase-conjugated anti-vWF antibody (Dakopatts P226) as the detecting antibody. The standard was a human pool of platelet-poor plasma (30 volunteers) that was assumed to contain 10 µg/mL of vWF. ELISAs were developed with o-phenylenediamine as the colorimetric substrate and quantified at A₄₉₀ on an ELISA reader (Molecular Devices, USA), as described previously.¹³

Synthesis of S-nitroso-AR545C peptide. S-nitrosation of AR545C was performed by 2 methods: (1) direct nitrosation by acidified NaNO₂,¹⁷ and (2) transnitrosation by the NO congener S-nitrosoglutathione (SNO-Glu).^{19,20} SNO-Glu was prepared within 5 minutes of use, kept at 4°C, and incubated with the purified AR545C fragment for 1 hour at an approximate 28:1 molar ratio (SNO-Glu:AR545C). The acidic pH of the mixture was then neutralized to pH 7.4 with NaOH and the unbound SNO-Glu was separated from the nitrosated AR545C (S-nitroso-AR545C) fragment by Sephadex G-25M (Pharmacia Biotech) column chromatography. The protein concentration of S-nitroso-AR545C was determined by the Coomassie Plus Protein Assay reagent (Pierce, Rockford, IL). The formation of the S-nitroso-AR545C peptide was confirmed by the Saville method²¹ and UV-visible spectroscopy.¹⁹ In the Saville method, NO is displaced from the S-nitrosothiol group with Hg²⁺ and assayed by diazotization of sulfanilamide with subsequent coupling to the chromophore N-(1-naph)-ethylenediamine; absorbance at 540 nm is measured to determine S-NO concentration.²¹ In this method, the sample containing S-nitroso-AR545C was first mixed with 0.5% ammonium sulfamate in 0.4 N HCl for 1 minute to remove free NO₂⁻ or HNO₂ from the sample. The S-nitroso content was calculated according to a standard curve constructed with 2.5 to 20 µmol/L NaNO₂.

UV-visible absorbance spectroscopy. Spectra were recorded at room temperature on a Cary 4E UV Visible spectrophotometer (Varian, Inc, Australia Pty, Ltd). Recorded spectra represent the absorbance of S-nitrosated AR545C compared with nonnitrosated AR545C.

Preparation of platelet-rich plasma (PRP). After obtaining informed consent, 9 vol of peripheral blood from healthy adult volunteers

was drawn into 1 vol of 0.129 mol/L trisodium citrate. After centrifugation (150g, 15 minutes, 22°C), the supernatant PRP was separated by removing the top two thirds of the plasma layer. Platelet-poor plasma (PPP) was prepared by centrifugation of PRP at 1,200g for 10 minutes and used immediately.

Preparation of gel-filtered platelets (GFP). GFP were obtained by passing PRP over a Sepharose-2B column (Pharmacia Biotech) in Tyrode's-HEPES-buffered saline as previously described.²² Platelet counts were determined using a Coulter Counter, model Technicon H2 (Bayer Diagnostics, Tarrytown, NY).

Cyclic nucleotide assay. Measurements of cGMP were performed using an ELISA methodology using anti-cGMP antiserum (Amersham Pharmacia Biotech, Uppsala, Sweden). cGMP was extracted from platelets as previously described.²³ Briefly, 10% trichloroacetic acid (TCA) was added to PRP before (negative control) and 5 minutes after the addition of SNO-Glu (positive control), AR545C, or S-nitroso-AR545C. Samples were vortexed, placed on ice, and centrifuged (8,000g, 4 minutes) at room temperature. The supernatant was extracted 4 times with diethyl ether and assayed for cGMP as above. Acetylation of samples with acetic anhydride was used to increase the sensitivity of the cGMP assay.

Effect of AR545C or S-nitroso-AR545C on ristocetin-induced platelet agglutination. Ristocetin-induced platelet agglutination was performed using lyophilized, formalin-fixed platelets (Helena Hemostasis, Beaumont, TX) as described previously.¹³ Various concentrations of either AR545C or S-nitroso-AR545C were incubated with the platelets (2 × 10⁸ platelets/mL) for 10 minutes in a platelet PACK-4 aggregometer (Helena Laboratories, Beaumont, TX) at 37°C before the addition of PPP as a source of vWF and 1.5 mg/mL of ristocetin (Sigma Chemical Co, St Louis, MO). The extent of agglutination was monitored to quantify the agglutination response.

Effect of AR545C or S-nitroso-AR545C on platelet aggregation. Platelet aggregation experiments were conducted using human PRP or GFP. Various concentrations of AR545C or S-nitroso-AR545C were incubated for 10 minutes with stirring at 37°C with PRP or GFP, and aggregation was induced with 5 µmol/L adenosine diphosphate (ADP). In some of the experiments, methylene blue (final concentration, 5 µmol/L) was added to the reactions containing S-nitroso-AR545C. Extent of aggregation was recorded in a PACK-4 aggregometer (Helena Laboratories).

Effect of AR545C or S-nitroso-AR545C on platelet interaction with extracellular matrix (ECM). Platelet adhesion and aggregation on ECM was tested in the cone-plate viscometer analysis system (Galai, Beit Ha'emek, Israel), as described previously.²⁴ In brief, 0.23 mL of citrated whole blood was placed on an ECM-covered plate under a shear rate of 1,300 s⁻¹ for 2 minutes. The sample was then washed and stained with May-Grünwald-Giemsa stain. Platelet adhesion and aggregation were determined using an image analysis system. The degree of adhesion was assessed by calculating the percentage of total area covered by platelets, and quantified as the percentage of surface coverage (SC); the normal value of SC is 19% ± 5.9% at this shear rate. The extent of platelet aggregation on the surface was estimated by measuring the frequency distribution of platelet aggregates of different size and the average size of ECM-bound platelet aggregates; the latter parameter is expressed as average size (AS) of the aggregates with the normal value of AS being 47.5 ± 15.2 µm² at this shear rate. To evaluate the effect of AR545C or S-nitroso-AR545C on the above-described parameters, the blood samples were preincubated at room temperature for 10 minutes with various concentrations of each of the peptides and the extent of adhesion and aggregation was recorded.

Effect of AR545C or S-nitroso-AR545C on botrocetin-induced aggregation of rabbit platelets ex vivo. All animals used in this study were approved by the Institutional Animal Care and Use Committee at the Neufeld Cardiac Research Institute (Sackler Faculty of Medicine, Tel Aviv University, Tel Aviv, Israel). New Zealand white female rabbits,

each weighing 2.5 to 3.0 kg, were anesthetized with intravenous sodium pentobarbital (Nembutal, 30 mg/kg, followed by 10 mg at 30- to 60-minute intervals) administered through the marginal ear vein. The auricular artery was cannulated for blood sampling. The rabbits were injected intravenously with 1 mg/kg AR545C ($n = 3$) or 0.5 mg/kg S-nitroso-AR545C ($n = 3$). In each animal, 3 mL blood was drawn before, and at various time intervals after, administration of the peptides. Eight parts of rabbit blood were drawn into 1 part of 0.129 mol/L trisodium citrate and rabbit PRP prepared. The effect of bolus injection of either AR545C or S-nitroso-AR545C on rabbit botrocetin-induced platelet aggregation was evaluated in an aggregometer (Helena Laboratories) as in the ristocetin-induced agglutination assay: 1 $\mu\text{g/mL}$ botrocetin (Sigma Chemical Co) was added to rabbit PRP containing 2×10^8 platelets/mL and 5 mmol/L EDTA at 37°C with stirring as described previously,¹³ and the extent of aggregation was then recorded. ADP-induced platelet aggregation experiments were performed using rabbit PRP and 5 $\mu\text{mol/L}$ ADP, and the extent of aggregation was recorded in a PACK-4 aggregometer (Helena Laboratories) as described above.

Coagulation tests and bleeding time. Prothrombin time (PT) and activated partial thromboplastin time (PTT) assays of rabbit plasma were performed using standard techniques. Innovin reagent (Dade, Miami, FL) was used for PT and Thrombosil I (Hemoliance Ortho Diagnostic Systems Inc, Raritan, NJ) or Actin FS (Dade) reagents were used for PTT. Bleeding time was measured as described previously.²⁵ Briefly, a shaved rabbit ear was placed into a 37°C saline bath for 5 minutes. A full-thickness standardized incision was made with a Surgicutt pediatric device (International Technique Corp, Edison, NJ). The ear was then returned to the saline bath, observed until all blood flow ceased, and the time recorded.

Statistical analysis. Statistical comparisons were performed using the 2-tailed Student's *t*-test for means and 2-way analysis of variance for dose-response. *P* values $< .05$ were considered significant. In the experiments with ECM comparison between AR545C and nitroso-AR535C, fragments for each dose were evaluated by 1-way analysis of variance (ANOVA). Ex vivo dose effect of the 2 fragments was evaluated by 2-way analysis of variance.

The synergism of the 2 agents was tested using isobole method for mutually exclusive and nonexclusive compounds as described previously.²⁶ For mutually exclusive compounds the isobole (*I*) representing the effect of the combination is calculated using the following formula: $I = (A/A_e) + (B/B_e) = 1$, where A_e and B_e are the corresponding doses of the individual compounds producing the same quantitative effect, and *A* and *B* are the doses of the compounds used in combination showing the same effect. For mutually nonexclusive drugs, the equation is changed to: $I = (A/A_m) + (B/B_m) + (A/A_m)(B/B_m) = 1$, where A_m and B_m represent the concentrations yielding the median effect. *I* is less than 1 when the compounds interact to produce synergistic effect.

RESULTS

Chemical analysis of S-nitroso-AR545C. Analysis of the formation of S-nitroso-AR535C performed by the method of Saville²¹ showed that the S-nitrosothiol content was 0.96 mol of S-NO/1 mol of AR545C. UV-visible spectroscopy of S-nitroso-AR545C compared with AR545C is presented in Fig 1. The characteristic 350-nm absorption peak of the S-nitrosothiol group of nitrosated AR545C is illustrated, confirming that the peptide was nitrosated. The additional absorption peak at 280 nm represents the protein content of the S-nitroso-AR545C. Absorption spectra of AR545C shows only the 280-nm peak characteristic for the peptide absorbance.

The putative structure of the S-nitrosated AR545C monomer is presented in Fig 2. It seems reasonable that the apparently free cysteine at residue 545 will be nitrosated; however,

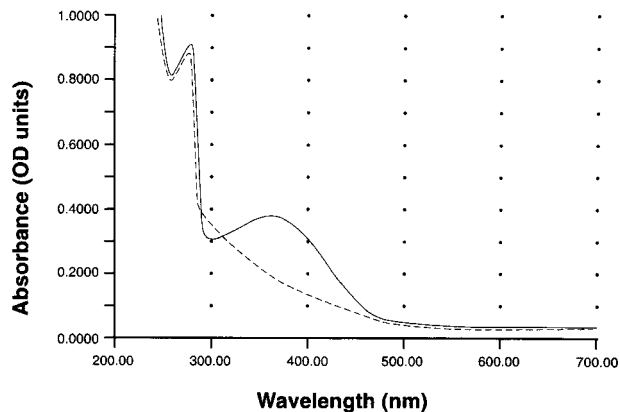


Fig 1. UV-Vis absorption spectra of S-nitroso-AR545C and AR545C. Spectra were recorded against a blank containing phosphate-buffered saline. Solid line indicates S-nitroso-AR545C; dashed line indicates AR545C.

additional cysteines of the molecule may be involved in the nitrosation process as well.

Effect of AR545C or S-nitroso-AR545C on ristocetin-induced platelet agglutination. Preincubation of human platelets with either AR545C or S-nitroso-AR545C resulted in inhibition of ristocetin-induced platelet agglutination in a dose-dependent manner. As shown in Fig 3, whereas 0.2 $\mu\text{mol/L}$ AR545C decreased agglutination by 40%, the same concentration of S-nitroso-AR545C completely abolished it. The concentration of AR545C required to inhibit ristocetin-induced agglutination by 50% (IC_{50}) was $0.1 \pm 0.03 \mu\text{mol/L}$, whereas the IC_{50} for S-nitroso-AR545C was $0.02 \pm 0.006 \mu\text{mol/L}$ ($P = .001$). Thus, S-nitrosation of AR545C inhibited platelet agglutination approximately 5-fold.

To test the effect of synergistic interactions between NO and AR545C, subthreshold concentrations of NO congener (SNO-Glu) and AR545C used alone or in combination with one another were added to PRP, and ristocetin-induced platelet aggregation was recorded in aggregometer. As shown in Fig 4, subthreshold concentrations of SNO-Glu or AR545C alone did not inhibit platelet aggregation. However, when the subthreshold concentrations of these agents were used in combination, inhibition of aggregation was obtained. Using an isobole method to establish synergy,²⁶ the isobole index for mutually

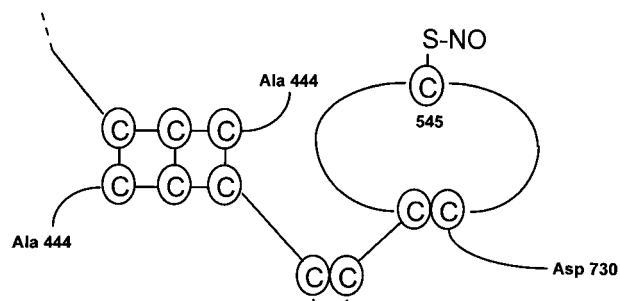


Fig 2. Structure of S-nitroso-AR545C. Note that the first 3 cysteines are depicted as disulfide-linked to their corresponding cysteines in a second monomer, only the partial structure of which is shown, as S-nitrosation was performed with the intact dimer.

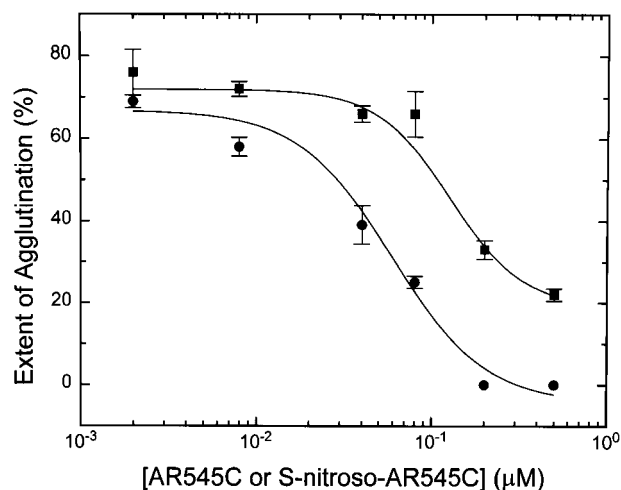


Fig 3. Dose-dependent ristocetin-induced inhibition of human platelet agglutination by S-nitroso-AR545C and AR545C. Formalin-fixed platelets (2×10^8 /mL) were incubated with either AR545C (■) or S-nitroso-AR545C (●) for 10 minutes at various concentrations followed by addition of normal PPP and 1.5 mg/mL ristocetin.

exclusive and nonexclusive compounds was calculated for each combination. When combination of 0.08 $\mu\text{mol/L}$ AR545C with 0.2 $\mu\text{mol/L}$ or 0.5 $\mu\text{mol/L}$ of SNO-Glu was analyzed, isobole indices of 0.57 and 0.81, respectively, were obtained. Similarly, combination of 0.2 $\mu\text{mol/L}$ AR545C with 0.2 $\mu\text{mol/L}$ or 0.5 $\mu\text{mol/L}$ SNO-Glu revealed isobole indices of 0.41 and 0.53, respectively. Thus, the result of this analysis showed that all the isobole indices were below 1, indicating synergy.

Effect of AR545C or S-nitroso-AR545C on ADP-induced platelet aggregation. The effects of AR545C or S-nitroso-AR545C were first studied in gel-filtered platelets and confirmed in PRP experiments. Results of aggregation experiments are provided in Fig 5. AR545C did not affect platelet aggregation. In contrast, dose-dependent inhibition of ADP-induced

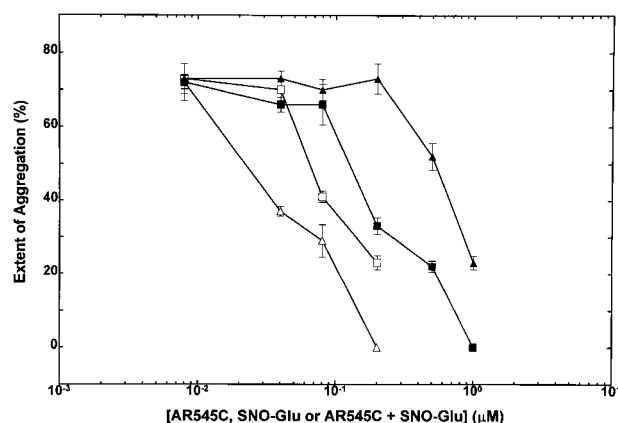


Fig 4. Inhibition of human ristocetin-induced platelet aggregation: Dose-response to combination of SNO-Glu and AR545C. Human PRP (2.5×10^8 /mL) was incubated with increasing concentrations of AR545C followed by addition of 1.5 mg/mL ristocetin in the absence (■) or presence of 2 concentrations of SNO-Glu: (□), 0.2 $\mu\text{mol/L}$ SNO-Glu; (Δ), 0.5 $\mu\text{mol/L}$ SNO-Glu. (\blacktriangle), Increasing concentrations of SNO-Glu in the absence of AR545C. Each point represents mean \pm SEM of 3 experiments.

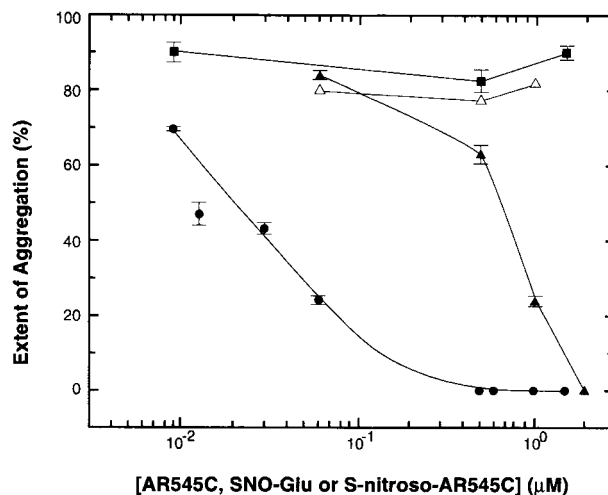


Fig 5. Dose-dependent inhibition of human ADP-induced platelet aggregation by S-nitroso-AR545C. Human PRP (2.5×10^8 /mL) were incubated with increasing concentrations of S-nitroso-AR545C (●), AR545C (■), or SNO-Glu (Δ), and aggregation was induced with 5 $\mu\text{mol/L}$ ADP. (Δ), Aggregations obtained after addition of methylene blue (final concentration, 5 $\mu\text{mol/L}$) to the mixture of PRP and S-nitroso-AR545C.

platelet aggregation was observed with S-nitroso-AR545C, with an $\text{IC}_{50} = 0.018 \pm 0.002$ $\mu\text{mol/L}$. Platelet aggregation was completely inhibited by S-nitroso-AR545C at concentrations above 0.5 $\mu\text{mol/L}$. This inhibition was reversed by addition of 5 $\mu\text{mol/L}$ methylene blue, cGMP inhibitor (Fig 5, Δ). NO congener SNO-Glu inhibited ADP-induced platelet aggregation only at concentrations above 1 $\mu\text{mol/L}$ (Fig 5, \blacktriangle).

Effect of AR545C or S-nitroso-AR545C on platelet cGMP. Normal PRP was incubated with 1.5 $\mu\text{mol/L}$ SNO-Glu (positive control), 0.5 $\mu\text{mol/L}$ AR545C, or 0.5 $\mu\text{mol/L}$ S-nitroso-AR545C, the platelet proteins were precipitated with TCA, and the protein-free supernatant was assayed for cGMP content as described in Materials and Methods. Compared with PRP alone (1.7 ± 0.4 pmol/ 10^9 platelets, negative control), addition of AR545C did not significantly alter basal cGMP level (2.4 ± 0.3 pmol/ 10^9 platelets) ($P = .19$) (Table 1). In contrast, there was a significant increase in cGMP levels with the addition of SNO-Glu or S-nitroso-AR545C ($P < .0001$ for each compound compared to AR545C) (Table 1). Thus, the increases in platelet cGMP levels after platelet exposure to SNO-Glu or S-nitroso-AR545C correlate with the inhibition of platelet aggregation by the effect of NO molecules provided by these compounds.

Effect of AR545C or S-nitroso-AR545C on platelet interaction with ECM. Normal whole blood tested in the cone-plate viscometer analysis system exhibited a typical adhesion and

Table 1. Platelet cGMP Content

	Control	SNO-Glu (1.5 $\mu\text{mol/L}$)	AR545C (0.5 $\mu\text{mol/L}$)	S-nitroso-AR545C (0.5 $\mu\text{mol/L}$)
pmol/ 10^9 platelets	1.7 ± 0.4	16 ± 0.5	2.4 ± 0.2	$8.3 \pm 0.2^{\dagger}$

Values represent mean \pm SEM of 3 determinations, each performed in duplicate.

* $P < .0001$ compared with control.

$\dagger P < .0001$ compared with AR545C.

aggregation pattern with surface coverage of $28.4\% \pm 5.9\%$ and an average size of the aggregates of $47.2 \pm 15.2 \mu\text{m}^2$ (Table 2). The normal blood sample was then preincubated for 10 minutes at room temperature with increasing concentrations of AR545C or S-nitroso-AR545C. As shown in Table 2, a dose-dependent inhibition of adhesion (represented by surface coverage) and aggregation (represented by average size of the aggregates) was observed with either fragment compared to control. However, the inhibitory effect of S-nitroso-AR545C was significantly more pronounced at concentration above $1.0 \mu\text{mol/L}$. A representative picture shown in Fig 6 demonstrates that incubation of normal blood (Fig 6A) with $1.5 \mu\text{mol/L}$ AR545C resulted in a 74% decrease in adhesion and 64% inhibition in aggregate formation (Fig 6B). Similar concentration of S-nitroso-AR545C resulted in complete inhibition of both adhesion and aggregate formation (Fig 6C). Analysis of the frequency distribution of aggregate sizes shows that S-nitroso-AR545C significantly shifted the size distribution leftward compared with control blood and with AR545C (Fig 6D through F). Thus, a more marked antiplatelet effect of S-nitroso-AR545C compared with AR545C was observed in these experiments, both with respect to inhibition of adhesion and aggregation under conditions of high shear.

Effect of AR545C or S-nitroso-AR545C on botrocetin or ADP-induced aggregation of rabbit platelets ex vivo. Rabbits were injected with 1 mg/kg AR545C or 0.5 mg/kg S-nitroso-AR545C (3 in each group), and the effect on ex vivo botrocetin or ADP-induced rabbit platelet aggregation was monitored, as shown in Figs 7 and 8. In animals injected with AR545C, the aggregation induced by botrocetin was significantly inhibited in a time-dependent manner, reaching a maximal effect 45 minutes after injection. The inhibitory effect was completely reversed by 2 hours after the injection. By contrast, in animals injected with S-nitroso-AR545C at one half the dose of AR545C, botrocetin-induced aggregation was completely abolished 45 minutes after the injection and the inhibitory effect persisted, showing 60% inhibition 2 hours after injection (Fig 7) ($P < .0001$ by 2-way ANOVA). AR545C had no effect on ADP-induced platelet aggregation (data not shown), but S-nitroso-AR545C exhibited time-dependent inhibition of platelet aggregation, reaching a maximal effect (almost 60% inhibition) at 1 hour after the injection and persisting for 1 additional hour (Fig 8).

Effect of AR545C or S-nitroso-AR545C on hemostatic parameters in rabbits. The hemostatic parameters measured before and at different time intervals after the injections of AR545C or S-nitroso-AR545C are presented in Table 3. No change in the platelet count, PT, or PTT values was observed. However, prolongation of the bleeding time was noted in both groups.

Twofold prolongation of bleeding time was observed 1 hour after injection in the group treated with AR545C that normalized after 2 hours. The prolongation of bleeding time was significantly greater in the group treated with S-nitroso-AR545C, increasing almost 8-fold compared with the pretreatment value. The bleeding time shortened by the end of the experiment but was still prolonged at 2 hours after injection.

DISCUSSION

Several agents have been shown to block the interaction between vWF and its platelet receptor GPIb.⁸⁻¹² Some of these compounds, such as monoclonal antibodies,^{5,9} synthetic peptides,²⁷ and recombinant vWF fragments,^{12,13} have been tested in various models of experimental thrombosis. In addition, it has previously been shown that NO or its S-nitroso-congeners exhibit antiplatelet properties by inhibiting platelet aggregation^{14,15} and adhesion.¹⁶

In our previous study,¹³ we showed that recombinant vWF fragment AR545C inhibited ristocetin- and botrocetin-induced platelet aggregation of human and rabbit platelets, respectively. AR545C also enhanced the thrombolytic effect of recombinant tissue-type plasminogen activator in a rabbit thrombosis model. In the present study, we evaluated the antiplatelet properties of the S-nitroso-derivative of AR545C, which should combine both antiadhesive actions with antiaggregating actions in the same molecule and target the delivery of NO to the site of vascular injury.

Our data show that S-nitroso-AR545C potentiated the antiplatelet effects of AR545C in the 3 systems studied: ristocetin- or botrocetin-induced platelet aggregation in vitro or ex vivo, ADP-induced platelet aggregation, and interaction of platelets with ECM under conditions of high shear. The superior antiplatelet effect of S-nitroso-AR545C can be attributed to the independent action of 2 moieties of the molecule: blocking platelet GPIb receptor through the AR545C moiety and elevating platelet cGMP through the -SNO moiety. Moreover, the data showed that these 2 effects are synergistic.

S-nitroso-AR545C inhibited ristocetin-induced platelet agglutination in a dose-dependent manner with an average $\text{IC}_{50} = 0.02 \pm 0.006 \mu\text{mol/L}$; this concentration is one fifth of that for AR545C.¹³ Similarly, in the cone-plate viscometer analysis system, a dose-dependent inhibition of adhesion and aggregation on ECM was more notable at each concentration of S-nitroso-AR545C compared with AR545C, reaching a statistically significant difference at concentrations greater than $1.0 \mu\text{mol/L}$ ($P < .05$ by ANOVA). Moreover, $1.0 \mu\text{mol/L}$ of S-nitroso-AR545C resulted in complete inhibition of aggregate

Table 2. Effect of AR545C or S-nitroso-AR545 on Platelet Interaction With ECM Under Flow Conditions

	Control	AR545C			S-nitroso-AR545C		
		0.5 $\mu\text{mol/L}$	1.0 $\mu\text{mol/L}$	1.5 $\mu\text{mol/L}$	0.5 $\mu\text{mol/L}$	1.0 $\mu\text{mol/L}$	1.5 $\mu\text{mol/L}$
Surface coverage (%)	28.4 ± 5.9	12.9 ± 1.1	10.0 ± 1.4	7.5 ± 1.8	10.2 ± 0.9	$5.5 \pm 1.3^*$	$4.8 \pm 1.1^*$
					$P = .09\ddagger$	$P = .05\ddagger$	$P = .004\ddagger$
Average size of aggregates (μm^2)	47.2 ± 15.2	36.2 ± 8.1	21.4 ± 5.7	17.1 ± 1.1	18.7 ± 2.2	$13.0 \pm 3.1^*$	$11.5 \pm 0.7^*$
					$P = .07\ddagger$	$P = .2\ddagger$	$P = .003\ddagger$

Results are expressed as mean \pm SEM of 3 determinations.

* $P < .05$ compared with control.

†Compared with the same concentration of AR545C.

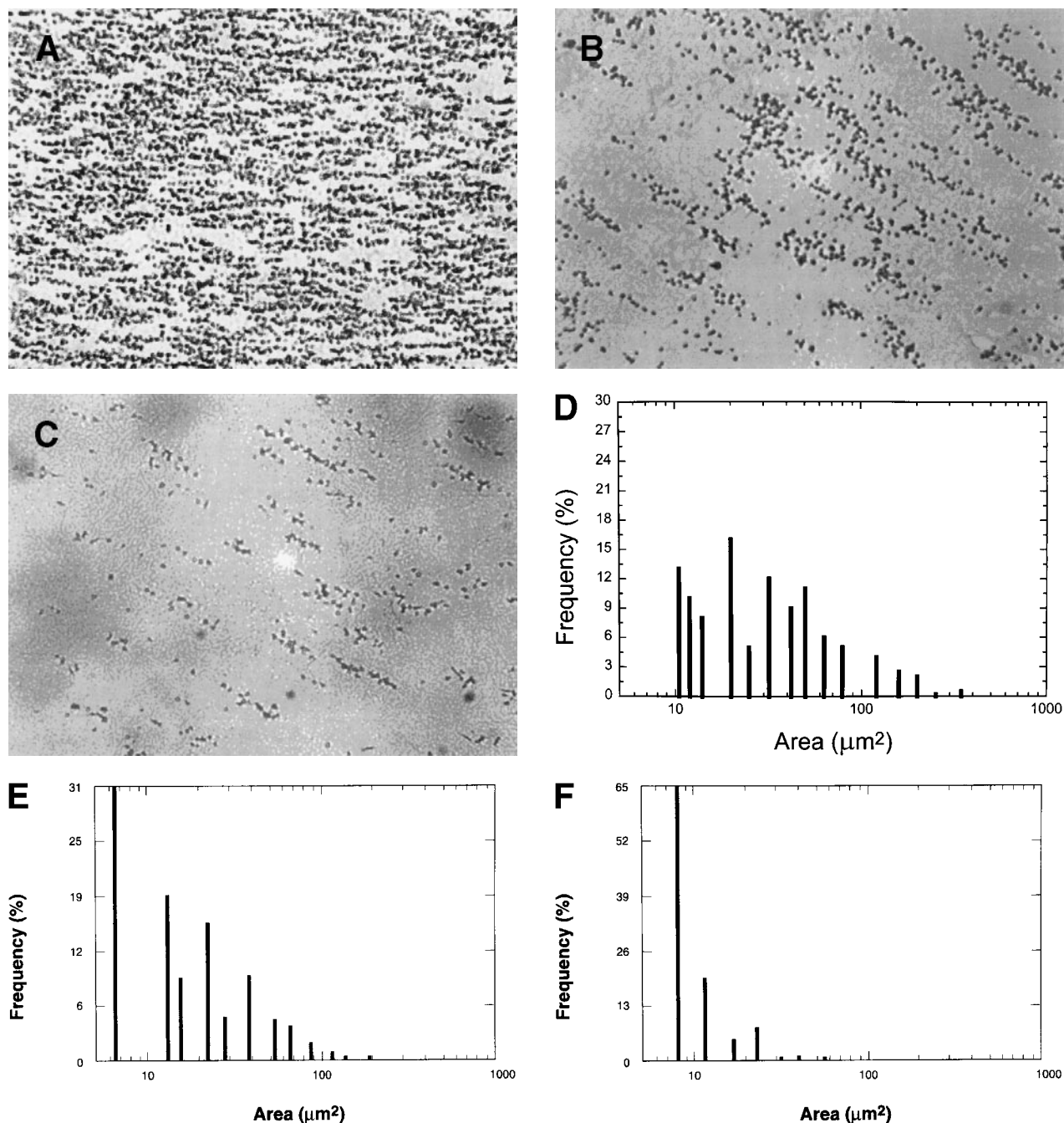


Fig 6. The effect of the S-nitroso-AR545C or AR545C on platelet interaction with ECM under flow conditions (shear rate of $1,300 \text{ s}^{-1}$). Citrated whole blood (0.25 mL) was tested in the cone-plate viscometer analysis system after a 10-minute preincubation with either control buffer, 1.5 $\mu\text{mol/L}$ AR545C, or 1.5 $\mu\text{mol/L}$ S-nitroso-AR545C, and shown in representative field of the video screen (A, B, and C, respectively). The corresponding frequency histograms (D, E, and F, respectively) for the size distribution of the adhered platelets and platelet aggregates are also depicted.

formation, whereas the same concentration of R545C had only a slight effect on aggregate formation.

As expected, AR545C showed no effect on ADP-induced platelet aggregation, because its effects are a consequence of competition with vWF for binding to GPIb. By contrast, a significant dose-dependent inhibition of ADP-induced platelet aggregation was observed with S-nitroso-

AR545C abolished platelet aggregation completely at concentrations greater than 0.5 $\mu\text{mol/L}$, and the IC_{50} was $0.018 \pm 0.002 \mu\text{mol/L}$. Finally, the ex vivo efficacy of S-nitroso-AR545C was examined in rabbits. At concentrations one half that of AR545C, S-nitroso-AR545C was able to inhibit significantly botrocetin-induced platelet aggregation to a much greater extent and for a longer period of time than AR545C itself, probably reflecting

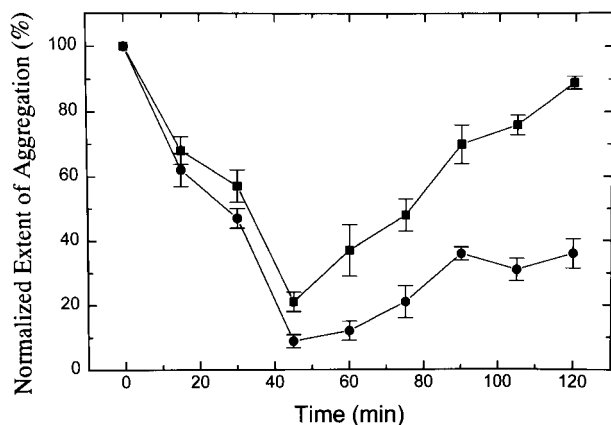


Fig 7. Effect of S-nitroso-AR545C or AR545C on rabbit platelet aggregation ex vivo. Female rabbits were injected with 0.5 mg/kg of S-nitroso-AR545C or 1 mg/kg AR545C intravenously (3 in each group). Blood samples were drawn before and at different time intervals after the injection. Platelet aggregation was induced ex vivo with 1 μ g/mL botrocetin added to PRP prepared from animals treated with AR545C (■) or S-nitroso-AR545C (●) and plotted relative to the pretreatment values. Results are expressed as mean \pm SEM values for $n = 3$ animals in each group.

the synergistic effect of NO with the vWF fragment. In addition, ADP-induced platelet aggregation was inhibited by S-nitroso-AR545C by almost 60%. Taken together, the potencies of the S-nitroso-AR545C in vitro and ex vivo appear to be significantly greater (3- to 10-fold and 4-fold, respectively) than those of AR545C.

The doses of AR545C or S-nitroso-AR545C used in this study had no effect on platelet count or plasma coagulation tests (PT, PTT); however, bleeding time was significantly prolonged, especially when rabbits were injected with the S-nitroso-AR545C, apparently because of its dual inhibitory effects on platelet function. Despite the prolongation in bleeding time, no bleeding was observed during the experiment or at necropsy of

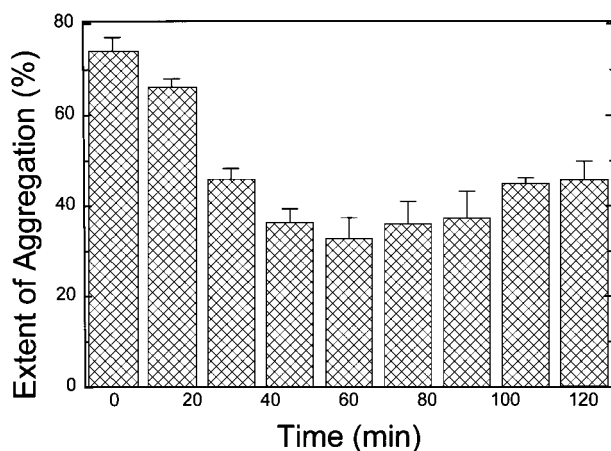


Fig 8. Effect of S-nitroso-AR545C on rabbit platelet aggregation ex vivo. Female rabbits were injected with 0.5 mg/kg S-nitroso-AR545C and blood samples were collected before and at different time intervals after the injection. Platelet aggregation was induced in PRP with 5 μ mol/L ADP. Results are expressed as mean \pm SEM for $n = 3$ animals.

Table 3. Effect of Intravenous AR545C or S-nitroso-AR545C Injection on Hemostatic Parameters in Rabbits

Time (min)	Bleeding Time (s)		
	0	60	120
(normal range)	(58-73)		
AR545C	62 \pm 2	130 \pm 11	90 \pm 20
S-nitroso-AR545C	63 \pm 5	483 \pm 17*	260 \pm 10*
	PT (s)		
Time (min)	0	60	120
(normal range)	(10.8-11.2)		
AR545C	11.0 \pm 0.1	10.6 \pm 0.2	10.8 \pm 0.3
S-nitroso-AR545C	11.0 \pm 0.2	10.8 \pm 0.1	10.7 \pm 0.4
	PTT (s)		
Time (min)	0	60	120
AR545C	11.8 \pm 0.9†	11.9 \pm 0.6†	12.8 \pm 0.1†
(normal range)	(10.1-13.3)†		
S-nitroso-AR545C	15.5 \pm 0.5‡	16.5 \pm 0.2‡	15.2 \pm 0.3‡
(normal range)	(14.6-16.3)‡		
	Platelets ($\times 10^9/L$)		
Time (min)	0	60	120
(normal range)	(355-468)		
AR545C	379 \pm 22	403 \pm 10	435 \pm 12
S-nitroso-AR545C	446 \pm 11	400 \pm 18	399 \pm 17

Results are mean \pm SEM values of 3 animals.

* $P < .001$ compared with control ($t = 0$) or AR545C.

†Measured with Thrombosil I or ‡Actin FS as described in Materials and Methods.

the animals. The prolongation of bleeding time observed in our study contrasts with the lack of effect on bleeding time reported by Azzam et al¹² after injection of VCL in guinea pigs. This difference may stem from differences in the model or the compound used.

Most drugs interfering with platelet function exhibit a single antiplatelet action, such as inhibition of adhesion or of aggregation. In contrast, S-nitroso-AR545C manifests 2 independent but synergistic antiplatelet activities combined in the same molecule. This compound likely has 2 pharmacologically relevant mechanisms in target cells: it may act through interference of platelet binding to vWF and through NO-mediated intracellular soluble guanylyl-cyclase activation. The data from this study show that S-nitroso-AR545C exhibits significantly more potent antiplatelet activity than AR545C, and this effect seems to be attributed to its independent actions via GPIb- and NO-dependent pathways.

ACKNOWLEDGMENT

We thank Stephanie Tribuna and Ann Ward Scribner for excellent technical assistance. We are indebted to David Castel, DVM, for his assistance in experiments with rabbits.

REFERENCES

- Sadler JE: von Willebrand factor. *J Biol Chem* 266:22777, 1991
- Ruggeri ZM, Zimmerman TS: von Willebrand factor and von Willebrand disease. *Blood* 70:895, 1987
- Fuster V, Bowie EW, Lewis JC, Fass DN, Owen CA Jr, Brown AL: Resistance to arteriosclerosis in pigs with von Willebrand disease. Spontaneous and high cholesterol diet-induced arteriosclerosis. *J Clin Invest* 61:722, 1978
- Nichols TC, Bellinger DA, Johnson TA, Lamb MA, Griggs TR:

von Willebrand's disease prevents occlusive thrombosis in stenosed and injured porcine coronary arteries. *Circ Res* 59:15, 1986

5. Bellinger DA, Nichols TC, Read MS, Reddick RL, Lamb MA, Brinkhous KM, Evatt BL, Griggs TR: Prevention of occlusive coronary artery thrombosis by a murine monoclonal antibody to porcine von Willebrand factor. *Proc Natl Acad Sci USA* 84:8100, 1987
6. Ikeda Y, Handa M, Kawano K, Kamata T, Murata M, Araki Y, Anbo H, Kawai Y, Watanabe K, Itagaki I, Sakai K, Ruggeri ZM: The role of von Willebrand factor and fibrinogen in platelet aggregation under varying shear stress. *J Clin Invest* 87:1234, 1991
7. Andrews RK, Gorman JJ, Booth WJ, Corino GL, Castaldi PA, Berndt MC: Cross-linking of a monomeric 39/34-kDa disperse fragment of von Willebrand factor (Leu-480/Val-481-Gly-718) to the N-terminal region of the alpha-chain of membrane glycoprotein Ib on intact platelets with bis (sulfosuccinimidyl) suberate. *Biochemistry* 28:8326, 1989
8. Fujimura Y, Titani K, Holland LZ, Russell SR, Roberts JR, Elder JH, Ruggeri ZM, Zimmerman TS: von Willebrand factor. A reduced and alkylated 52/48-kDa fragment beginning at amino acid residue 449 contains the domain interacting with platelet glycoprotein Ib. *J Biol Chem* 261:381, 1986
9. Cadroy Y, Hanson SR, Kelly AB, Marzec UM, Evatt BL, Kunicki TJ, Montgomery RR, Harker LA: Relative antithrombotic effects of monoclonal antibodies targeting different platelet glycoprotein-adhesive molecule interactions in nonhuman primates. *Blood* 83:3218, 1994
10. Golino P, Ragni M, Cirillo P, Pascucci I, Ezekowitz MD, Pawashe A, Scognamiglio A, Pace L, Guarino A, Chiariello M: Aurintricarboxylic acid reduces platelet deposition in stenosed and endothelially injured rabbit carotid arteries more effectively than other antiplatelet interventions. *Thromb Haemost* 74:974, 1995
11. Strony J, Song A, Rusterholtz L, Adelman B: Aurintricarboxylic acid prevents acute rethrombosis in a canine model of arterial thrombosis. *Arterioscler Thromb Vasc Biol* 15:359, 1995
12. Azzam K, Garfinkel LI, Bal dit-Sollier C, Cisse Thiam M, Drouet L: Antithrombotic effect of a recombinant von Willebrand factor, VCL, on nitrogen laser-induced thrombus formation in guinea pig mesenteric arteries. *Thromb Haemost* 73:318, 1995
13. Gurevitz O, Goldfarb A, Hod H, Feldman M, Shenkman B, Varon D, Eldar M, Inbal A: Recombinant von Willebrand factor fragment AR545C inhibits platelet aggregation and enhances thrombolysis with rtPA in a rabbit thrombosis model. *Arterioscler Thromb Vasc Biol* 18:200, 1998
14. Stamler J, Mendelsohn ME, Amarante P, Smick D, Andon N, Davies PF, Cooke JP, Loscalzo J: N-acetylcysteine potentiates platelet inhibition by endothelium-derived relaxing factor. *Circ Res* 65:789, 1989
15. Cooke JP, Stamler J, Andon N, Davies PF, McKinley G, Loscalzo J: Flow stimulates endothelial cells to release a nitrovasodilator that is potentiated by reduced thiol. *Am J Physiol* 259:H804, 1990
16. de Graaf JC, Banga JD, Moncada S, Palmer RMJ, de Groot PG, Sixma JJ: Nitric oxide functions as an inhibitor of platelet adhesion under flow conditions. *Circulation* 85:2284, 1992
17. Stamler JS, Simon DI, Osborne JA, Mullins ME, Jaraki O, Michel T, Singel DJ, Loscalzo J: S-nitrosylation of proteins with nitric oxide: Synthesis and characterization of biologically active compounds. *Proc Natl Acad Sci USA* 89:444, 1992
18. Ruggeri ZM: von Willebrand factor as a target for antithrombotic intervention. *Circulation* 86:26, 1992 (suppl 3)
19. Zhang Y-Y, Xu A-M, Nomen M, Walsh M, Keaney JF Jr, Loscalzo J: Nitrosation of tryptophan residue(s) in serum albumin and model dipeptides. Biochemical characterization and bioactivity. *J Biol Chem* 271:14271, 1996
20. Mendelsohn ME, O'Neill S, George D, Loscalzo J: Inhibition of fibrinogen binding to human platelets by S-nitroso-N-acetylcysteine. *J Biol Chem* 265:19028, 1990
21. Saville B: A scheme for the colorimetric determination of microgram amounts of thiols. *Analyst* 83:670, 1958
22. Hawiger J, Parkinson S, Timmons S: Prostacyclin inhibits mobilisation of fibrinogen-binding sites on human ADP- and thrombin-treated platelets. *Nature* 283:195, 1980
23. Butt E, Walter U: Cyclic nucleotides: Measurement and function, in Watson SP, Authi KS (eds): *Platelets. A Practical Approach*. Oxford, UK, Oxford University Press, 1996, p 259
24. Varon D, Dardik R, Shenkman B, Kotev-Emeth S, Farzame N, Tamarin I, Savion N: A new method for quantitative analysis of whole blood platelet interaction with extracellular matrix under flow conditions. *Thromb Res* 85:283, 1997
25. Johnstone MT, Andrews T, Ware JA, Rudd MA, George D, Weinstein M, Loscalzo J: Bleeding time prolongation with streptokinase and its reversal with 1-desamino-8-D-arginine vasopressin. *Circulation* 82:2142, 1990
26. Collen D: Synergism of thrombolytic agents: Investigational procedures and clinical potential. *Circulation* 77:731, 1988
27. Mohri H, Zimmerman TS, Ruggeri ZM: Synthetic peptides inhibit the interaction of von Willebrand factor-platelet membrane proteins. *Peptides* 14:125, 1993